Phys. cond. Matter 19, 405—416 (1975)

Fermi Surface Studies of Non-Dilute Disordered Alloys by Positron Experiments*

Stephan Berko and Jan Mader**
Brandeis University, Waltham, Massachusetts, USA

The technique of positron annihilation experiments as applied to the study of Fermi surfaces in metals and alloys is briefly reviewed. The angular correlation of the two annihilation photons is directly related to the momentum distribution of the positron-electron system; breaks in this distribution reflect the size and shape of the Fermi surface. Recent two-dimensional angular correlation measurements designed to study the Fermi surface of Cu-Al and Cu-Zn alloys are presented, and are compared with theoretical predictions.

Introduction

It is well known that the high precision techniques used to measure the Fermi surfaces (FS) of pure metals, such as the de Haas-van Alphen effect, magnetoresistance, etc., cannot be applied to the study of high concentration disordered alloys; because of electron lifetimes these FS measurements are limited to below $\sim 1\%$ atomic concentration solutes.

There exist other FS techniques, not requiring long electronic lifetimes. Neutron inelastic scattering, based on the "Kohn anomaly" in the phonon dispersion curves, can measure in principle some features of the FS even in disordered alloys [1]; the technique, however, is mainly useful if the FS possesses parallel flat regions. The Kohn anomaly can also be observed in diffuse x-ray scattering and has been used to measure the size of the FS in the $\langle 110 \rangle$ direction in Cu-Al alloys [2]. An other recent development is the use of the polar reflection Faraday effect by Tracy and Stern, who have measured the FS shapes of several Ag based disordered alloys [3].

The physics of positron (e^+) interactions in solids has been intensively studied during the last decade [4] and has been applied to study various features of the electronic band structure of solids. In particular the angular correlation between the two photons emitted when a e^+ annihilates in a solid reflects the momentum distribution of the positron-electrons system; thus the size and shape of the FS can be studied. Although the positron annihilation technique cannot compete in precision with the standard measurements of FS-s in pure metals, it can yield information about the shape as well as the sharpness of the FS in non-dilute alloys [5].

In this paper we present a brief review of positron experiments in general and illustrate the present state of art with some recent results in Cu-Al and Cu-Zn alloys.

---

* Work supported by the National Science Foundation and the U. S. Army Research Office, Durham.

** Gillette Fellow 1972—1974.

Positron Annihilation Experiments

In the typical e^+ experiment a beam of positrons from a radioactive source is injected into the solid to be studied; the e^+ slows down to low velocities well before it annihilates; one is thus concerned with a thermalized (or nearly thermalized [6]) e^+ annihilating with the electrons in the solid. Several techniques exist to study the nature of the electrons the e^+ annihilated with: (1) two-photon angular correlation measurements, (2) energy measurements of the annihilation photons, (3) e^+ lifetime experiments, and (4) $2\gamma/3\gamma$ yield measurements. The two-photon angular distribution measurements measure the e^+-e^- momentum density and are most often used for FS studies. The energy measurement, through the Doppler effect, also reflects the momentum distribution, but because of inherent energy resolution limitations, it is less frequently used. The e^+ lifetime depends on the local density of electrons at the e^+ site, and is thus a sensitive measure of the effective e^+-e^- interaction. Finally $2\gamma/3\gamma$ yield measurements are important when the spins of the e^+ and e^- are not random, such as in the case of ferromagnetic studies using polarized positrons. We will focus our attention on the 2γ angular correlation measurements.

The Theory of Two-Photon Angular Correlation Experiments

The angular correlation between the two annihilation photons (2γ) from singlet e^+-e^- overlaps reflects the momentum distribution $\varrho(\boldsymbol{p})$ of the e^+-e^- system. In Fig. 1 we have sketched the geometry of the typical 2γ correlation measurement. One finds that for a typical atomic momentum $\boldsymbol{p}$ the angle between the two photons is nearly 180°. For a given detector set at C_1 the second time-coincident photon will hit the counter plane C_2 at coordinates θL and φL, where L is the distance to the annihilation source. From energy and momentum conservation $\theta = p_z/mc$ and $\varphi = p_y/mc$ to within a high precision. The third component gives rise to a Doppler shift of the photons. Thus an ideal measurement of angles θ and φ as well as of the photon energy can yield $\varrho(\boldsymbol{p})$ directly. Because of counting rate problems, one usually uses long detectors, thus integrating over one component, say p_y, without energy measurement. Such a "long-slit" geometry measures in principle $N(p_z) = \int\int \varrho(\boldsymbol{p})\, dp_x\, dp_y$. Given sufficient counting rates, one can use small counters in coincidence ("point-slit" or "crossed-slit" geometry), thus measuring $N(p_y, p_z) = \int \varrho(\boldsymbol{p})\, dp_x$. The actual measured counting rates correspond to the folding of these integrals into the geometrical resolution given by the slit widths, the sample size, the finite temperature effect, etc.

In the bottom drawing of Fig. 1 we indicate the measurement by the two different geometries for the simple case of a spherical free electron Fermi momentum distribution; in the "long-slit" case one obtains counting rates proportional to planar slices in momentum space perpendicular to the one component measured (p_z); in the "point-slit" geometry, the coincidence rate is proportional to a chord as indicated by the shaded region. For this simple case one predicts for the long-slit geometry an inverted parabolic angular distribution in $\theta = p_z/mc$, with the cut-offs θ_F measuring the Fermi momentum $p_F = \theta_F mc$; for the two-dimensional case one predicts circular distributions with cut-off depending on the value of $\varphi = p_y/mc$. A typical Fermi momentum in metals corresponds to $\theta_F \sim 4$—6 milli-

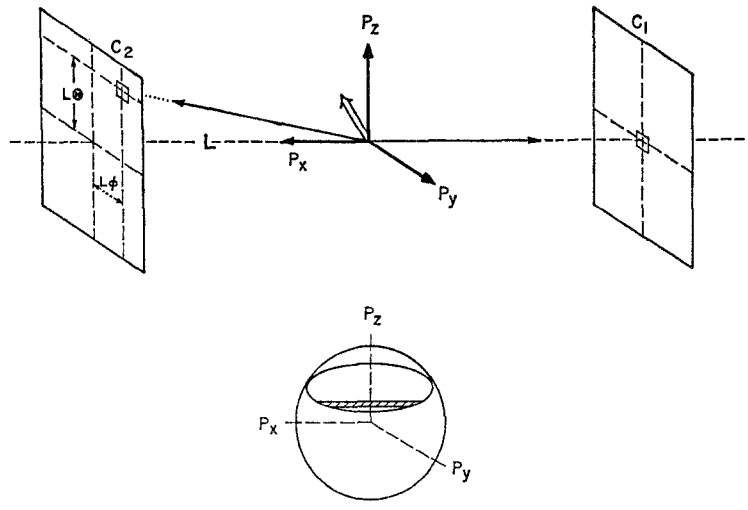

Fig. 1. Geometry of the two-photon angular correlation experiment (not to scale). Typically, angles θ and φ are a few milliradians

radians (one milliradian equals a momentum of $mc \times 10^{-3}$, i.e. 0.137 in atomic units).

In the independent particle approximation (IPM), the probability of annihilation photons to carry away momentum $\boldsymbol{p}$, within the range $d\boldsymbol{p}$, is given for a e^+ annihilating in a periodic crystalline solid at zero temperature by the e^+—e^- momentum density

$$\varrho(\boldsymbol{p}) = \text{Const.} \sum_{k,n} \left| \int d^3\boldsymbol{r} \exp(-i\,\boldsymbol{p}\cdot\boldsymbol{r})\, \psi_{k^+}(\boldsymbol{r})\, \psi_{k,n}(\boldsymbol{r}) \right|^2, \tag{1}$$

where $\psi_{k^+}(\boldsymbol{r})$ is the ground state positron wavefunction, and $\psi_{k,n}$ is the electron wavefunction with wavenumber $\boldsymbol{k}$ (crystal momentum) and band index n; the summation is over all occupied states $\boldsymbol{k}, n$ ($\hbar \equiv 1$, in the units used, $\boldsymbol{k}$ is in the first [reduced] zone). Since one deals with a single e^+ ground state, we set $\boldsymbol{k}^+ = 0$, i.e., $\psi_{k^+}(\boldsymbol{r}) = u_0^+(\boldsymbol{r})$; $\psi_{k,n}(\boldsymbol{r}) = u_{k,n}^-(\boldsymbol{r}) \exp(i\,\boldsymbol{k}\cdot\boldsymbol{r})$. From Eq. (1) we obtain the partial momentum density $\varrho_{k,n}(\boldsymbol{p})$ from $\varrho(\boldsymbol{p}) = \sum_{k,n} \varrho_{k,n}(\boldsymbol{p})$

$$\varrho_{k,n}(\boldsymbol{p}) = \text{Const.} \sum_{\boldsymbol{G}} \left| A_{\boldsymbol{G}}(\boldsymbol{k}, n) \right|^2 \delta(\boldsymbol{p} - \boldsymbol{k} - \boldsymbol{G}), \tag{2}$$

where the $\boldsymbol{G}$-s are the reciprocal lattice vectors of the crystal and $A_{\boldsymbol{G}}(\boldsymbol{k}, n)$ is the coefficient in the expansion of the periodic function

$$u_0^+(\boldsymbol{r})\, u_{k,n}^-(\boldsymbol{r}) = \sum_{\boldsymbol{G}} A_{\boldsymbol{G}}(\boldsymbol{k}, n) \exp(i\,\boldsymbol{G}\cdot\boldsymbol{r}).$$

As discussed in an early paper by Berko and Plaskett [7] Eq. (2) shows the fundamental difference between real momentum $\boldsymbol{p}$ and crystal momentum $\boldsymbol{k}$: an electron with quantum number $\boldsymbol{k}$ will contribute not only at $\boldsymbol{p} = \boldsymbol{k}$, but at all $\boldsymbol{p} = \boldsymbol{k} + \boldsymbol{G}$, with amplitude $|A_{\boldsymbol{G}}(\boldsymbol{k}, n)|^2$. Thus, when summing over all occupied states $\boldsymbol{k}, n$ in a metal, the momentum distribution will exhibit breaks not only

at the Fermi surface in the first zone ($\boldsymbol{p} = \boldsymbol{k}$) but, due to the higher momentum components (HMC) of the e^+ and e^- wavefunctions, these breaks reoccur in higher zones ($\boldsymbol{p} = \boldsymbol{k} + \boldsymbol{G}$, $\boldsymbol{G} \neq 0$, the so-called "Umklapp annihilations"). One thus obtains a sequence of "FS" shapes in momentum space, as in the repeated zone scheme, but modulated by the $|A_{\boldsymbol{G}}|^2$-s. The measurement of $\varrho(\boldsymbol{p})$ via the angular correlation curves thus contains two sets of information: (a) sharp *breaks* in $\varrho(\boldsymbol{p})$ reflect the topology of the FS, whereas (b) the actual complete *shape* of the correlation curves measures the nature of the wavefunctions via the $|A_{\boldsymbol{G}}(\boldsymbol{k}, n)|^2$-s. One of the problems in interpreting the angular distribution is to be able to separate these two effects; this can be achieved reasonably successfully for simple metals, but for complicated FS topologies it could become a major difficulty.

The various theoretical problems connected with evaluating $\varrho(\boldsymbol{p})$ can be divided into several categories: (a) the evaluation of $u_0^+(\boldsymbol{r})$ and $\psi_{\boldsymbol{k},n}(\boldsymbol{r})$ in various band model approximations within the IPM, (b) the many-body effects of e^+-e^- correlations due to the Coulomb interaction, and (c) the effect of finite temperature on $\varrho(\boldsymbol{p})$.

The positron wavefunction is usually obtained by standard solid state techniques as a Bloch wave at $\boldsymbol{k} = 0$, by inverting the sign of the electronic potentials; Wigner-Seitz approximation [7], plane wave expansion [8] and a modified KKR technique [9] were used in various metals.

A different approximation for the e^+ wavefunction was recently introduced by Kubica and Stott [10]; they express the actual e^+ wavefunction as a product of a Wigner-Seitz function and e^+ "pseudo-wavefunction", which then is plane-wave expanded. This method is particularly useful in discussing the behavior of the e^+ in alloys. Stott and Kubica [11], in a study of the e^+ affinity to the various constituents in an alloy conclude that, although the e^+ can have strong preference for one type of atom rather than for the other, it is very unlikely that any particular atom can form a bound state with the positron.

The question of the importance of the e^+-e^- interaction in the full many-body treatment has been studied by several authors [4]. In effect, the interaction does not change substantially the predictions of the IPM model: for the NFE-like metals the e^+-e^- Coulomb interaction has the effect of enhancing the annihilation probability as one approaches the FS. This enhancement has been observed experimentally in the alkali metals [4]. Recently, computations by Fujiwara [12] on two-level systems indicate the possibility that the Coulomb interaction has also the effect of reducing the magnitude of the HMC-s. The most important theoretical findings for the FS measurements is that the Coulomb interactions and the other many-body effects do not change the breaks in $\boldsymbol{p}$ space from the positions of the Fermi surface [4]. Thus one can measure directly FS dimensions without having to invoke theoretical computations.

The effect of finite temperature on $\varrho(\boldsymbol{p})$ is taken into account by folding the zero temperature expression [Eq. (2)] into the appropriate statistical temperature factors. It can be easily shown that the effective temperature smearing at the FS breaks is governed mainly by the positron thermal motion. For a free e^+ mass at room temperature, for example, this smearing corresponds to ≈ 0.5 mrad. The many-body e^+-e^- correlations introduce an increase in the e^+ effective mass m^* (the IPM e^+ band mass is close to m_0, the free e^+ mass), measured to be

$(1.8 \pm 0.2)\, m_0$ in Na [6]. Thus, the theoretical limitation on the ultimate momentum space resolution obtainable by e^+ experiments is governed by the e^+ thermal motion. Another important effect which can lead to deviations in $\varrho(\boldsymbol{p})$ from Eq. (1) is the probability of e^+ trapping at crystal defects [4], particularly vacancies and dislocations. The vacancy captured e^+-s overlap less with core electrons, and one observes a decrease in $\varrho(\boldsymbol{p})$ for high momentum, where core electrons contribute substantially, accompanied by a corresponding increase at low momenta. The capture of e^+-s by vacancies has been extensively used recently as an important new technique of measuring the thermal activation energies of vacancies in metals [13].

Another technique used to measure momentum densities in solid is the Compton profile measurement [14]. Because these measurements are not perturbed by the e^+'s presence they are more useful in principle when studying general momentum density shapes; on the other hand, because of better resolution, the e^+ technique is used in the measurements of the sharp breaks of the momentum densities due to the presence of the Fermi surface. At present the attainable resolution in the Compton measurements using x rays is ≈ 1.3 mrad (≈ 0.18 a.u.), but with γ rays, needed when studying high Z solids, the resolution becomes ≈ 3 mrad, compared to typical e^+ resolutions of 0.2—1 mrad.

Fermi Surface Measurements

For counting rate reasons, most angular correlation experiments have been performed with "long-slit" geometry. The method has been applied successfully to single crystal solids, such as Be, graphite, the alkali metals, Si and Ge, Cu, the rare earths, to ordered alloys such as V_3Si and even to ferromagnetic systems [4]. Briefly, one finds that the angular distribution is indeed parabolic for simple metals having a nearly-free-electron-like conduction band, with a sharp break at the FS, superimposed on a broad momentum distribution which is due to annihilation with core electrons, as well as Umklapp annihilations with the HMC of the valence band. Mijnarends [15] has shown that it is also feasible to obtain mathematically the three-dimensional (anisotropic) density $\varrho(\boldsymbol{p})$ from a set of experimental $N(p_z)$ curves, where p_z is taken along several crystallographic orientations.

We now turn to the application of the e^+ technique to the study of Fermi surfaces in disordered alloys. One of the early alloy measurements was reported by A. T. Stewart on the Li-Mg system. Besides the swelling of the nearly spherical Fermi surface of Li upon alloying it with Mg, Stewart also reports a surprisingly large smearing of the momentum distribution near k_F in the alloy specimen. Both Stewart and Stern [16] attribute this effect to a possible pile up of electric charge around the magnesium ions leading to virtual electronic transition in $\boldsymbol{k}$ space.

Recently, however, the Li-Mg system has been re-studied by Kubica *et al.* [17] who point out the possibility of localized e^+ states around clusters of Li atoms, and use the e^+ pseudo-potential wavefunction model for the computation of the e^+ affinity to Li vs Mg.

Because of the e^+ affinity to crystal defects [13], most experiments performed with polycrystalline samples are somewhat suspect, and we turn to experiments

using single crystal alloys. The most intensively studied alloy systems to date are the copper based alloys. Fujiwara and Sueoka [18] were the first to observe the copper $\langle 111 \rangle$ neck in $\varrho(\boldsymbol{p})$ by using a crossed-slit geometry apparatus, thus reducing the contribution of core electrons. They were able to compensate for the automatic loss in counting rate in going to crossed-slits by producing e^+ radioactive ^{64}Cu internally by neutron irradiation of the copper single crystals.

Since this measurement, several high precision experiments have been performed on copper, comparing the angular distributions directly with details of the Fermi surface. In particular, it was shown by Berko, Cushner, and Erskine [19] and by Mijnarends [20] that the shape of the FS can be also observed with the standard long-slit geometry apparatus. In Ref. 19 the question of the importance of the shape of the FS compared to the details of the wavefunctions in $\varrho(\boldsymbol{p})$ was studied, by finding the extent to which the long-slit geometry data reflected simply the variation of cross-sectional areas due to planar cuts of the FS.

A technique different from either the long-slit or crossed-slit angular distribution, and particularly suited to the observation of the FS necks, is the so-called "rotating specimen method", introduced independently by Sueoka and Williams *et al.* [4]. In this method the counters, with crossed-slits, are kept co-linear, i.e., at 180° ($\theta = 0$, $\varphi = 0$, Fig. 1), and the single crystal sample is rotated with respect to the counter axis. These "rotation curves" correspond to a measure of $N(p_z, p_y)_{p_z=p_y=0}$, at various orientations of the crystal axis. When the single crystal Cu is rotated about the $\langle 110 \rangle$ axis, the $\langle 111 \rangle$ necks are made evident. This technique, however, does not contain the same amount of information as do angular distributions along various directions. If one could neglect the rather complicated contributions of HMC, and if one could subtract uniquely the core distribution, the method would provide a measurement proportional to the diameter of the Fermi surface along the direction of the counter axis.

Using the various methods discussed so far several investigators have reported measurements in copper-based high concentration disordered alloys. Most experimentalists have concentrated in measuring the size of the $\langle 111 \rangle$ neck radius with alloying. We shall select a few recent examples indicating the present precision attainable, and compare the results with available theoretical predictions.

In Fig. 2 we plot the $\langle 111 \rangle$ neck radii in milliradians ($mc \times 10^{-3}$ units with $\hbar \equiv 1$) against the electron per atom (e/a) ratio for α-brass, as obtained by Morinaga [21] and by Williams [22] using the rotating specimen method, by Becker *et al.* [23] using crossed-slit geometry, and by Triftshäuser and Stewart [24] using long-slit geometry apparatus. We notice that the error bars are typically $\pm$ (0.1—0.2) mrad corresponding to a $\approx 10\%$ accuracy in neck radii. In Ref. 23 a discussion is presented showing the problems encountered in analyzing the "rotating specimen" results. These problems might well lead to systematic errors which could explain the somewhat lower values obtained by this technique.

In Fig. 2 we have also plotted for comparison three recent theoretical predictions by Bansil *et al.* [25]. The curve marked RB is a rigid band prediction based on a KKR calculation of the Cu band structure, with a crystal potential generated by the renormalized atom approach. The curves marked CR and SMT have been obtained from an average t-matrix calculation of the energy bands for disordered brass, with charge transfer having been incorporated by two different methods:

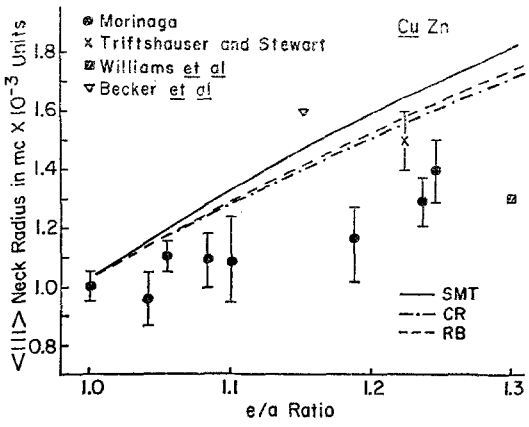

Fig. 2. The radius of the ⟨111⟩ FS neck of copper and of α-brass as a function of e/a ratio measured by various positron techniques. The theoretical curves are discussed in the text

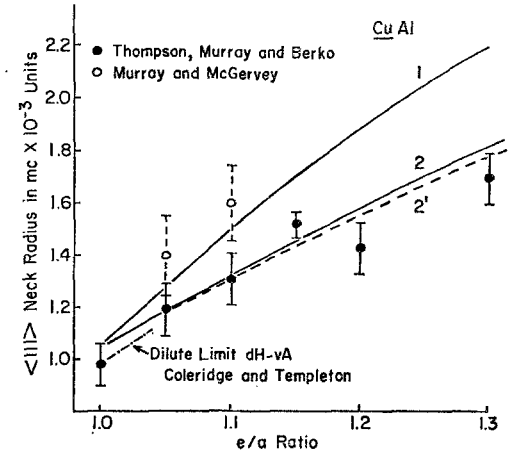

Fig. 3. The ⟨111⟩ FS neck radius for Cu-Al alloys. The theoretical curves are discussed in the text

charge renormalization (CR) and the shifted muffin tin (SMT) model. All three curves have been corrected for the change in lattice parameter upon alloying, using the calculation of Davis, Faulkner and Joy [26] for the band structure of copper as a function of lattice spacing. The differences between the theoretical curves indicate the precision that will be needed before the neck measurements can differentiate between the various theoretical models.

In Fig. 3 we plot the results for the ⟨111⟩ neck in the Cu-Al system, measured by Murray and McGervey [27] and by Thompson, Murray and Berko [28] by the long-slit method. The early result by Fujiwara, Sueoka and Imura [29], indicating a non-monotonic behavior, has not been plotted, since in a recent paper by Akahane *et al.* [30] these earlier results are not confirmed, and a monotonic behavior is found. The theoretical curve marked 1 in Fig. 3 corresponds to the

early RB prediction by Ziman based on his eight-cone model of the copper FS. The curves 2 and 2′ are the RB predictions of Bansil *et al.* [25] with (2′), and without (2) lattice expansion correction, in order to exhibit the magnitude of such a correction. In Ref. 30 the FS along the ⟨100⟩ direction has also been measured, indicating no contact with the zone face for concentrations up to 15.5 at.% Al.

From Fig. 3 we see that the ⟨111⟩ neck follows the RB prediction based on an up-to-date copper band computation quite well. The fact, however, that the neck measurements are consistent with rigid band does not necessarily mean that the copper bands are simply filling up on alloying. Rea and De Reggi [31] have recently developed a band model for Cu-Al, in order to explain their optical measurements in which the conduction band sinks with respect to the *d* bands on alloying Cu with Al, similarly to the earlier model invoked by Lettington [32] for Cu-Zn alloys.

Fermi surfaces have also been measured in the Cu-Ge and Cu-Ga systems by McLarnon and Williams [33] and Hasegawa *et al.* [34] and in Cu-Ga and Cu-Si by Suzuki *et al.* [35]. No contact with the (200) zone face was found in Cu-Ga.

Measurements have been performed on Cu-Ni alloys by several groups [4], but so far the results seem uncertain, and even contradictory, perhaps due to the problems encountered with growing good homogeneous Cu-Ni single crystals. The experiment also becomes harder because the ⟨111⟩ neck decreases upon alloying with nickel.

Recent Experiments with a New Multicounter Angular Correlation Apparatus

In order to improve the precision of the FS measurements by the positron technique higher counting rates and better resolution are required. To avoid the necessity of producing *in situ* ^{64}Cu sources by neutron activation that can lead to possible radiation damage, as well as to be able to study solids not containing copper, we have built a crossed-slit system using a multiple counter array, and an external ^{58}Co source. At present 22 counters are used in pairs, with an effective (FWHM) resolution of ≈ 0.6 mrad along p_z, and ≈ 3 mrad along the p_y direction (see Fig. 1); these figures include the geometrical resolution as well as the e^+ thermal motion (at 100 K). To indicate the precision obtainable, we plot in Fig. 4 the angular correlation curve $N(p_y, p_z)$ obtained in copper with a crystal orientation designed to study the Fermi vector along the [110] direction (K_{110}). The first and second derivatives with respect to p_z are also shown. The position of the zero crossing of the second derivative, after correction for the shift due to the resolution function, yields the Fermi vector. The broad momentum distribution beyond the Fermi break is due to core electrons and Umklapp annihilations with the conduction band. The same geometry was used to study K_{110} in Cu-Al alloys. Our results are plotted in Fig. 5. Also plotted are the points measured by the x-ray diffuse scattering observation of the Kohn anomaly [2]. The solid and dashed curves marked RB are the rigid band computations with and without lattice correction, and the RS curves correspond to the simple rigid scaling model used in Ref. 2. The comparison of the angular distributions in Cu-Al with the distribution in pure Cu shows no evidence of a FS smearing in the alloys used, within our present accuracy of $\approx 5\%$ of K_{110}.

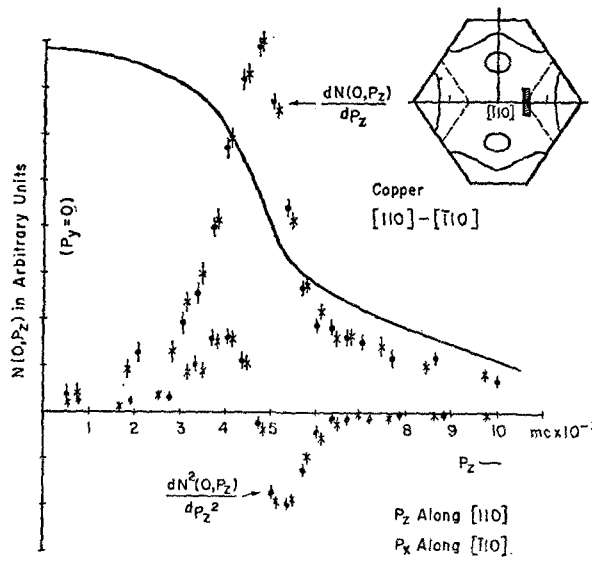

Fig. 4. $N(p_y, p_z)_{p_y=0}$ curve for copper and the first and second derivatives with respect to p_z. The crosses correspond to data for $p_z < 0$, with proper change in sign. The insert is the projection of the FS and the BZ onto the $p_y p_z$ plane, indicating the orientation of the crystal. The mark on the horizontal axis of the insert corresponds to 4 mrad

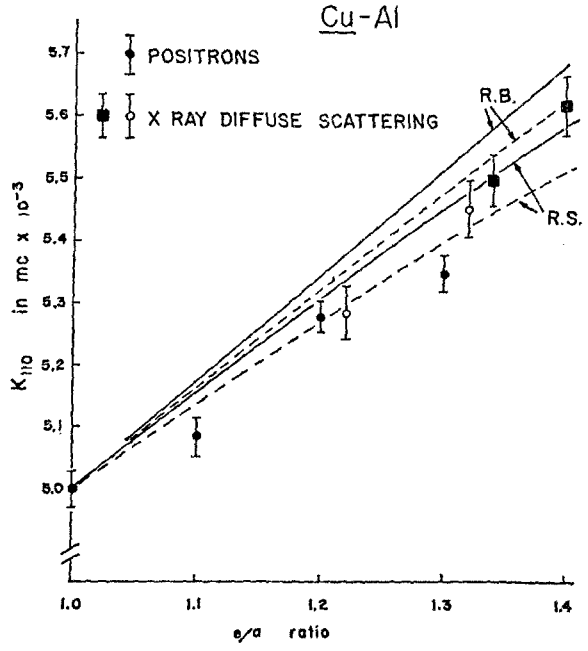

Fig. 5. The Fermi vector K_{110} vs e/a for Cu-Al alloys obtained by positron annihilation and by x-ray diffuse scattering. The theoretical curves are discussed in the text

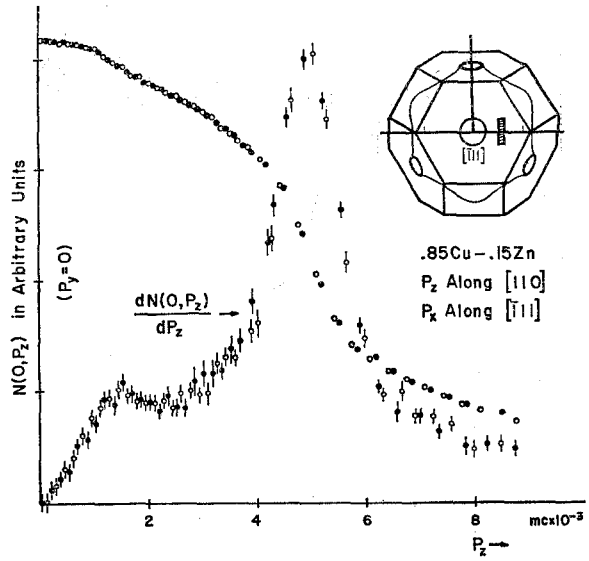

Fig. 6. $N(p_y, p_z)_{p_y=0}$ curve for 0.85 Cu- 0.15 Zn and the first derivative with respect to p_z. The open circles correspond to data for $p_z < 0$ (with proper change in sign for the derivative). The insert is the projection of the FS and the BZ onto the $p_y p_z$ plane, indicating the orientation of the crystal. The mark on the horizontal axis of the insert corresponds to 4 mrad

Finally in Fig. 6 we plot the angular correlation obtained recently in a .85 Cu-.15 Zn alloy, using an orientation that allows the measurement of the $\langle 111 \rangle$ neck. The effect of the neck can be clearly seen in the derivative curve, also plotted. Using these curves, a preliminary estimate yields for the $\langle 111 \rangle$ neck radius (1.45 $\pm$ 0.10) mrad, compared to the pure copper neck of 1 mrad. We also obtain from the curve the value of $K_{110} = 5.20 \pm .05$ mrad. Both values are somewhat smaller than the ones reported by Becker *et al.* [23] for the same Zn concentration. The measured neck value agrees well with the (SMT) theoretical prediction of Ref. 25 (see Fig. 2).

Conclusion

We have seen that positron annihilation experiments can be used to measure the FS of high concentration disordered alloys. The experiments indicate that, for the alloy systems studied, the FS is well defined and does not show appreciable smearing. As indicated, however, the positron technique is not without some genuine problems, stemming mainly from the e^+ affinity to lattice defects and structural inhomogeneities in general. Thus the major problem facing the FS measurements in disordered alloys by e^+ annihilation is the quality of the single crystals obtainable. Great care will have to be taken in understanding the role of vacancy-impurity interaction, the preferential annihilation with one of the solutes, the importance of cluster formation, etc. Future angular correlation experiments will have to be accompanied by detailed lifetimes studies on the samples to ascertain that the positrons annihilate mostly with a single lifetime

and are thus not trapped partially in defects or around preferential solute sites. In spite of the limitations, it should be possible to reduce the present uncertainties in the FS measurements by a factor of 5—10, by increasing the number of counters and using better angular resolution. With such improvements the smearing of the FS due to electron lifetimes effects will become measurable along different orientations, thus making more direct contact with the high precision electron lifetime measurements in dilute alloys, the main subject of this conference.

Acknowledgements. We thank Drs. A. Bansil, S. C. Moss, and L. Schwartz for important discussions regarding parts of this paper, and we are grateful to Dr. G. Beardsley for many valuable discussions and for the critical reading of our manuscript.

References

1. See for example Powell, B. M., Martel, P., Woods, A. D. B.: Phys. Rev. **171**, 727 (1968)
2. Scattergood, R. O., Moss, S. C., Bever, M. B.: Acta metallurgica **18**, 1087 (1970) Gaudig, W., Warlimont, H.: Z. Metallk. **60**, 488 (1969)
3. Tracy, J. M., Stern, E. A.: Phys. Rev. B **8**, 582 (1973)
4. See the up-to-date review by West, R. N.: Advances in Phys. **22**, 263 (1973)
5. For a more detailed review of e^+ Application to Alloy Studies, see the article by Berko, S., Charge Transfer-Electronic Structure of Alloys (Met. Soc. of AIME, New York 1974), p. 319—342
6. Kim, S. M., Stewart, A. T., Carbotte, J. P.: Phys. Rev. Letters **18**, 385 (1967)
7. Berko, S., Plaskett, J. S.: Phys. Rev. **112**, 1877 (1958)
8. Stroud, D., Ehrenreich, H.: Phys. Rev. **171**, 399 (1968)
9. Mijnarends, P. E.: Physica **63**, 235 (1973)
10. Kubica, P., Stewart, A. T., Stott, M. J.: Appl. Phys, **3**, 417 (1974)
11. Stott, M. J., Kubica, P.: Phys. Rev. B **11**, 1 (1975)
12. Fujiwara, K., Hyodo, T., Ohyama, J.: J. Phys. Soc. Japan **33**, 1047 (1972)
13. See for example the review article by Seeger, A.: J. Phys. F **3**, 248 (1973), also Appl. Phys. **4**, 183 (1974)
14. See review articles by Cooper, M.: Advances in Phys. **20**, 453 (1971) and Reed, W. A., Eisenberger, P.: Charge Transfer-Electronic Structure of Alloys (Met. Soc. of AIME, New York 1974), p. 271—289
15. Mijnarends, P. E.: Phys. Rev. **160**, 512 (1967)
16. Stern, E. A.: Phys. Rev. **168**, 730 (1968)
17. Kubica, P., McKee, B. T. A., Stewart, A. T., Stott, M. J.: "Proceedings of the Second International Conference on Positron Annihilation", Kingston, Ontario (unpublished), p. 1.153; also Phys. Rev. B **11**, 11 (1975)
18. Fujiwara, K., Sueoka, O.: J. Phys. Soc. Japan **21**, 1947 (1966)
19. Berko, S., Cushner, S., Erskine, J. C.: Phys. Letters **27 A**, 668 (1968)
20. Mijnarends, P. E.: Phys. Rev. **178**, 622 (1969)
21. Morinaga, H.: J. Phys. Soc. Japan **33**, 996 (1972)
22. Williams, D. L., Becker, E. H., Petijevich, P.: Bull. Amer. Phys. Soc. **14**, 402 (1969)
23. Becker, E. H., Petijevich, P., Williams, D. L.: J. Phys. F **1**, 806 (1971)
24. Triftshäuser, W., Stewart, A. T.: J. Phys. Chem. Solids **32**, 2717 (1971)
25. Bansil, A., Ehrenreich, H., Schwartz, L., Watson, R. E.: Phys. Rev. B **9**, 445 (1974)
26. Davis, H. L., Faulkner, J. S., Joy, H. W.: Phys. Rev. **167**, 601 (1968)
27. Murray, B. W., McGervey, J. D.: Phys. Rev. Letters **24**, 9 (1970)
28. Thompson, A., Murray, B. W., Berko, S.: Phys. Letters **37 A**, 461 (1971)
29. Fujiwara, K., Sueoka, O., Imura, T.: J. Phys. Soc. Japan **24**, 467 (1968)
30. Akahane, T., Sueoka, O., Morinaga, H., Fujiwara, K.: J. Phys. Soc. Japan **36**, 135 (1974)
31. Rea, R. S., De Reggi, A. S.: Phys. Letters **40 A**, 205 (1972)
32. Lettington, A. H.: Phil. Mag. **11**, 863 (1965)

33. McLarnon, J. G., Williams, D. L.: private communication; see also Abstract A 12 of the "Third International Conference on Positron Annihilation", Otaniemi (1973)
34. Hasegawa, M., Suzuki, T., Hirabayashi, M., Yajima, S.: Acta Cryst. **A 28**, S 102 (1972)
35. Suzuki, T., Hasegawa, M., Hirabayashi, M.: Appl. Phys. **5**, 269 (1974)

S. Berko
Brandeis University
Waltham, Massachusetts 02154, USA

Discussion

Watts: You showed data in aluminum, with the points lying very nearly on the circle. Do you think the departure of the points from the circle represents the departure of the Fermi surface from being spherical or the transfer of higher momentum components?

Berko: We have quite a few experiments, along different orientations, and it is clear that all the departures can be explained by the momentum density rather than k density, that is, they are indeed wave function effects rather than a change in the Fermi surface. The break at the end of the circle is the one point that clearly depends on the position of the Fermi surface.